Research article

X-RAY SPECTROMETRY

Received: 29 September 2014 Revised: 13 January 2015 Accepted: 13 January 2015 Published online in Wiley Online Library: 19 February 2015

(wileyonlinelibrary.com) DOI 10.1002/xrs.2590

Examples of XRF and PIXE imaging with few microns resolution using SLcam® a color X-ray camera†

S. H. Nowak,[a]* A. Bjeoumikhov,[a,b] J. von Borany,[c] J. Buchriegler,[c] F. Munnik,[c] M. Petric,[d] A. D. Renno,[e] M. Radtke,[f] U. Reinholz,[f] O. Scharf,[a] L. Strüder,[g] R. Wedell[h] and R. Ziegenrücker[e]

We present results of recent development of the color X-ray camera, type SLcam®, allowing detection of X-ray images with few microns resolution. Such spectral resolution is achieved with the use of high-quality polycapillary optics combined with sub-pixel resolution. Imaging of Siemens star resolution test chart reveals that the resolution limit of SLcam® can go down to nearly 5 μm. Several real sample examples of measurements carried out at the laboratory, synchrotron, and particle-induced X-ray emission beamlines are shown. This is the first time SLcam® is used as particle-induced X-ray emission detector.

Introduction

X-ray fluorescence (XRF) or particle-induced X-ray emission (PIXE) spatially-resolved imaging is usually achieved by scanning techniques; either by scanning on a sample surface in both *x* and *y* directions a micro-focused X-ray beam (in case of XRF) or an ion micro-beam (in case of PIXE); or, in alternative, keeping the micro-beam fixed and moving the sample by high-precision XYZ-stage[1]. The X-ray or ion beam excite the sample's elements, which, after the recombination process, emit X-ray photons that are collected by energy-dispersive detectors. To reconstruct the spatial distribution, the spectrum at each mapping position has to be accessed either by altering the exciting beam position or moving the sample by high-precision XYZ-stage.

The spatial resolution of scanning systems is mainly restricted by the size of the beam. While the micro-focused X-ray tubes offer beam spots merely approaching tens of microns[2] the best synchrotron and PIXE facilities provide X-ray or ion beam spots of some hundreds of nanometers[3,4].

Despite indisputable pros of scanning-based imaging, this method has some limitations like as follows: time-consuming process of scanning over a large area of a sample, possible missing of localized inhomogeneities when probing with a step larger than the beam size, refocusing on uneven objects, and radiation damage issues due to the beam brilliance. In some special cases, the scanning cannot be effectively applied. This is the case for XYZ-stage scanning of liquid or fragile samples that cannot be agitated, or for Total Reflection XRF (TXRF) where spatially resolved measurements are hampered because of a largely elongated beam footprint on a sample[5].

An alternative approach suppressing the need for faster scanning consists of exciting the probe with a broad beam and recording the fluorescence photons with a position-sensitive, energy-dispersive detector performing a full-field analysis. With such a setup, it is possible to take an X-ray image of the whole investigated area of the sample at once with the first, low-statistics image visible immediately. This is a significant difference to scanning systems, where the full image is visible only after the end of a scan. Furthermore, there is no need for sample movement, and the requirements on beam size confinement are also withdrawn. As it will be shown, the spatial resolution of such a system can reach several microns. This is not competitive with ion beam or synchrotron nano-focused excitation; however, certainly better than micro-focus X-ray tubes used in table top scanning devices.

SLcam® - a color X-ray camera

SLcam®'s descriptive name 'Color X-ray Camera' is based on the fact that the device gives information not only on the signal

* *Correspondence to: Stanisław H. Nowak, IFG Institute for Scientific Instruments GmbH, Berlin, Germany. E-mail: nowak@ifg-adlershof.de*

† *Presented at the European Conference on X-Ray Spectrometry, Bologna, Italy, 15–20 June 2014*

a *IFG Institute for Scientific Instruments GmbH, Berlin, Germany*

b *Institute of Computer Science and Problems of Regional Management, Kabardino-Balkar Scientific Center, Russian Academy of Sciences, Nalchik, Russia*

c *Helmholtz-Zentrum Dresden-Rossendorf, Dresden, Germany*

d *Institut "Jožef Stefan", Ljubljana, Slovenia*

e *Helmholtz Institute Freiberg for Resource Technology, Helmholtz-Zentrum Dresden-Rossendorf, Freiberg, Germany*

f *BAM Federal Institute for Material Research and Testing, Berlin, Germany*

g *PNSensor GmbH, Munich, Germany*

h *IAP Institute for Applied Photonics e.V., Berlin, Germany*

intensity (brightness), but, similarly to color camera working in visible light, also on the energy of photons[6,7]. Accordingly, a color picture can be obtained by assigning different hues to different X-ray energies. If energies are chosen as characteristic lines of XRF, the elemental distribution of a sample is visualized. The hue can also be associated to the mean energy deposited in a pixel or to regions of interest defined by the spectrum channels. Such alternative coloring is especially useful in case of geological samples where differentiation between grains and domains is often as important as the actual elemental composition.

The operating principle of SLcam® is based on two factors: (1) an ultra fast pn-junction charge-coupled device (pnCCD) capable of single photon counting and (2) polycapillary optics guiding the X-ray photons from a small area on a probe to designated pixels on the pnCCD chip. Single photon counting allows determination of the energy and position of a photon while X-ray guiding provides gathering and transfer of X-ray photons preserving the spatial information. A dedicated software enables steering the camera and real time visualization of the hyper-spectral data cube (x, y, E) by displaying regional spectra, intensity maps of X-rays of chosen energies, and overlay images[6].

pnCCD

pnCCD is a special type of a charge-coupled device developed for simultaneous spectroscopy and imaging of X-rays [8]. The detector is characterized by its radiation hardness, high-quantum efficiency in the X-ray range, very good energy resolution, and high-frame rate capability. The unique property of pnCCD is its capability of precise determination of the amount of generated electrons in every pixel. Consequently, each pixel in the matrix acts as an individual energy-dispersive point detector.

The $12.7 \times 12.7\ mm^2$ pnCCD chip consists of $48 \times 48\ \mu m^2$ pixels in a 264×264 matrix. It is placed in a vacuum housing 6.5 mm below a 50-μm-thick Be-window. The 450 μm thickness of sensitive Si area provides quantum efficiency above 95% in the range from 3 to 10 keV (the lower limit is given by the Be-window) and clearly above 30% at 20 keV. The chip is cooled with a Peltier element to ensure a good energy resolution being below 160 eV for the Mn Kα line (5.9 keV). All pixels in a row are processed in parallel. In combination with fast electronics, a frame rate of 1000 Hz is reached[7]. Imaging is achieved using fast, multi-frame recording of separate photon events giving an energy spectrum at each pixel.

Sub-pixel resolution

When an X-ray photon is absorbed in a silicon layer, an electron cloud is generated with a number of electrons proportional to the photon energy. In most cases, the charge is split over several pixels. With a correct analysis of the charge distribution, sub-pixel coordinates of a photon hit can be retrieved[9].

Polycapillary optics

A standalone pnCCD can be used for imaging in cases where the spatial and angular radiation distribution is well defined, *e.g.* spatially resolved X-ray transmission[10], diffraction[11] or scattering measurements[12]. However, to acquire a spatially resolved image of a divergent X-ray source – which is the case for XRF and PIXE – an X-ray optics needs to be used to guide photons from small regions on a sample to corresponding pixels on the detector. In this respect, polycapillary optics [13] works as a bunch of independent X-ray channels gathering the photons from the X-ray source and bringing them to a proper section of the charge-coupled device.

The polycapillary optics is a bundle of glass tubes with a typical diameter of several microns separated by a thin wall. The principle of an X-ray polycapillary optics operation is based on the effect of total external reflection. For incidence angles below the critical angle of total reflection, the reflection coefficient reaches values near to 100%. X-ray radiation is guided through the optics being reflected at the inner surface of the capillary channels. This effect increases the angular acceptance, *i.e.* solid angle of accepted radiation, at the cost of additional beam spreading and, consequently, obtainable resolution.

The polycapillary objectives can be designed and manufactured with parallel straight channels ideal for 1:1 imaging. Alternatively, conical-shaped structures can be produced. In such optics, the entrance and exit diameter of individual channels differ allowing magnification or reduction of the transmitted image.

Experimental

Measurements were performed at XRF installations employing synchrotron radiation and X-ray tubes, and also at a PIXE facility. Two types of polycapillary lenses manufactured by IFG Institute for Scientific Instruments GmbH were used: a parallel 1:1 optics with a channel diameter of 20 μm, and a conical 8:1 magnifying optics with capillary entrance diameter of 2 μm. Resolution limits were estimated employing a Siemens star resolution test chart fabricated in Fraunhofer IZM. Performance of SLcam® imaging with sub-pixel resolution was assessed on several real samples.

XRF setup

The XRF measurements were performed with synchrotron radiation and laboratory X-ray tubes. The synchrotron source was provided at the BAM*line* facility at BESSY II [14]. The X-ray tube measurements were realized in the laboratory of the Institute for Applied Photonics in Berlin. In both cases, the source location and sample-camera distance and position were optimized for the best count rates and lowest image distortion. A detailed description of

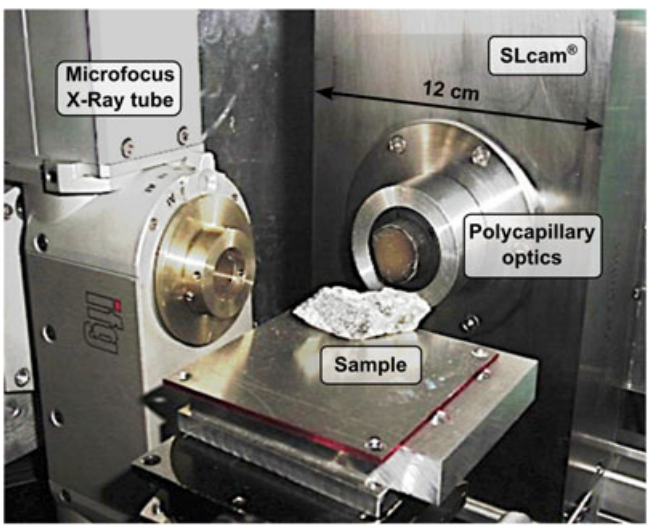

Figure 1. X-ray tube setup with 1:1 polycapillary optics at the laboratory of the Institute for Applied Photonics in Berlin.

both setups can be found in[6] and[15]. An example arrangement of the laboratory setup is shown in Figure 1.

High-Speed PIXE

High-Speed PIXE is a novel approach to the simultaneous analysis of a large area of mineral samples with sub 100 μm lateral resolution for resource technology applications. The new setup is developed at the Ion Beam Center at Helmholtz-Zentrum Dresden-Rossendorf, and combines broad beam proton excitation with a color X-ray camera SLcam®. The main aim of the beamline is the collection of multi-channel energy-dispersive spectra sensitive for trace element analysis.

The most important beam parameters for High-Speed PIXE are a high-proton current and a homogeneous illumination of the detection area. The first requirement is needed to maximize the X-ray yield and the latter to enable the quantification of element concentrations. The setup uses 3 MeV protons from a 6 MV tandem accelerator as excitation radiation. The maximal usable proton current at the PIXE endstation amounts to 1 μA. Two sets of horizontal and vertical slits in combination with two magnetic quadrupole lenses and a magnetic steerer can be used to optimize the beam shape and position on the sample.

To realize a homogeneous illumination of the analysis area ($12 \times 12\ mm^2$) the focused beam is moved very fast across the surface of the sample. The beam direction is altered by a two-dimensional (x, y) electrostatic scanning system comprising plates in horizontal and vertical orientation. By 'writing' Lissajous figures with frequencies of 1015 Hz (horizontal) and 1036 Hz (vertical), a homogeneous illumination is achieved within seconds for the entire detection area.

The geometry of the sample chamber (Figure 2) is optimized to ensure an undistorted PIXE image of the sample and a high X-ray yield. Therefore, the whole chamber is tilted 15° toward the beam. The induced X-rays are detected by SLcam® mounted parallel to the sample surface. Besides SLcam®, an optical polarization microscope is installed on top of the sample chamber with an offset of 150 mm. It can be used for sample inspection, orientation, and correlative microscopy. In order to limit the influence by any gas particles, the method requires a vacuum of better than 10^{-6} mbar.

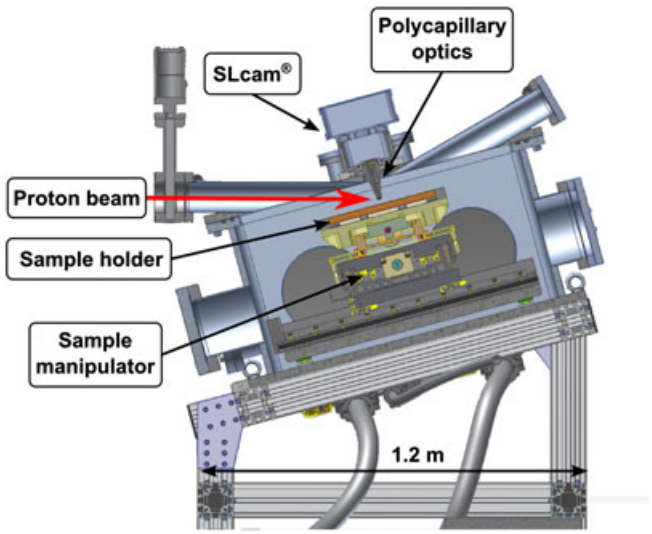

Figure 2. Cross section of the sample chamber at the High-Speed PIXE beamline at thelon Beam Center at Helmholtz-Zentrum Dresden-Rossendorf. PIXE, particle-induced X-ray emission.

Results

Siemens star

The Siemens star structure is deposited on an Si support and consists of concentric, evenly distributed Sn stripes and a small central disc used for alignment. Getting closer to the center, the stripes are becoming thinner and the spacing between them narrower. At a certain point, the dimensions are below the resolution limit, and the contrast between the structure and the support is too low to recognize the stripes. This is observed as a gray disc around the center of the Siemens star image. The radius of the gray disc L_{gray} can be used to calculate the resolution as the smallest resolvable detail:

$$R_{\mu m} = \frac{\pi L_{gray}}{N}, \quad (1)$$

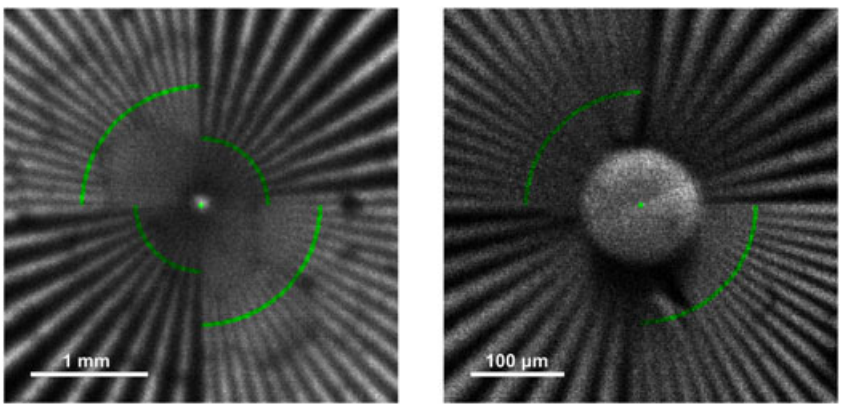

Figure 3. Images of an Sn Siemens star rendered with 4 × 4 sub-pixel division. The images represent the intensity of Sn L lines and were measured at: (left) High-Speed PIXE setup with 1:1 polycapillary optics with channel diameter of 20 μm (one pixel on the image corresponds to $12 \times 12\ \mu m^2$ area), and (right) TXRF setup with 8:1 focusing optics with channel entrance diameter of 2 μm (one pixel on the image corresponds to $1.5 \times 1.5\ \mu m^2$ area). The green lines indicate the borders of the gray disc area in which the contrast between the stripes and background is below 10%. PIXE, particle-induced X-ray emission; TXFR, total reflection X-ray fluorescence.

or as the highest number of resolvable line pairs per millimeter:

$$R_{LP} = \frac{N}{2\pi L_{gray}}, \quad (2)$$

where N is the number of stripes in the 2π angle.

At High-Speed PIXE beamline, the Siemens star was measured with a 1:1 objective; 8:1 focusing objective was used with the XRF setup. It should be noted that spatial resolution of SLcam® is determined by many factors such as the diameter of capillaries, acceptance angle, signal to noise ratio, and pixel dimensions. In order to prune the pixel size contribution, the Siemens star images were rendered with 4×4 sub-pixel division (see Figure 3). Accordingly, one pixel on analyzed sub-pixel images corresponds to 12×12 μm^2 area for 1:1 optics, and $1.5 \times 1.5\,\mu m^2$ area for 8:1 optics. This is below the corresponding capillary channel diameters.

The gray disc analysis of 4×4 sub-pixel images reveals resolution limits of 45 μm for the 1:1 optics and 5.4 μm for the 8:1 optics. This corresponds to a resolution of 11 and 93 line pairs per mm (LP/mm), respectively. Without sub-pixel rendering, the revealed resolution limits are noticeably worse (see Table 1).

Real samples

In the following, we present three examples of XRF and PIXE measurements on real samples. The first sample (see Figure 4) is a picoliter droplet of Ni solution [16]. The droplet was measured at synchrotron facility in TXRF geometry and with 8:1 magnifying optics. To demonstrate the image quality enhancement when sub-pixel resolution is employed, the SLcam® image is presented in standard resolution and with 4×4 sub-pixel division (see left and central panel in Figure 4). In the right panel in Figure 4, an atomic force microscopy picture of the droplet is presented for comparison. It can be noticed that the size of the droplet is slightly increased for the case of X-ray imaging. This might be an effect of the optics blur or the vagueness of the magnification factor.

Table 1. Comparison of two polycapillary optics and their use in measurements with and without sub-pixel division. The sub-pixel size is calculated from the 48 μm pixel size of the pnCCD chip divided by the magnification factor.

Optics name:	1:1		8:1	
Magnification:	1		8	
Field of view [mm^2]:	12×12		1.5×1.5	
Entrance [μm]:	20		2	
Exit [μm]:	20		16	
Pixel division:	1×1	4×4	1×1	4×4
Sub-pixel [μm]:	48	12	6	1.5
Resolution [μm]:	53	45	6.5	5.4
Resolution [LP/mm]:	9	11	77	93

pnCCD, pn-junction charge-coupled device

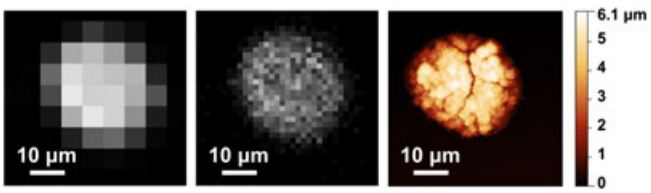

Figure 4. TXRF images of the Ni Kα fluorescence intensity of a picoliter droplet in standard (left) and 4×4 sub-pixel (center) resolution, and morphology of the droplet measured with atomic force microscopy (right). X-ray fluorescence was measured with 8:1 focusing optics. TXFR, total reflection X-ray fluorescence.

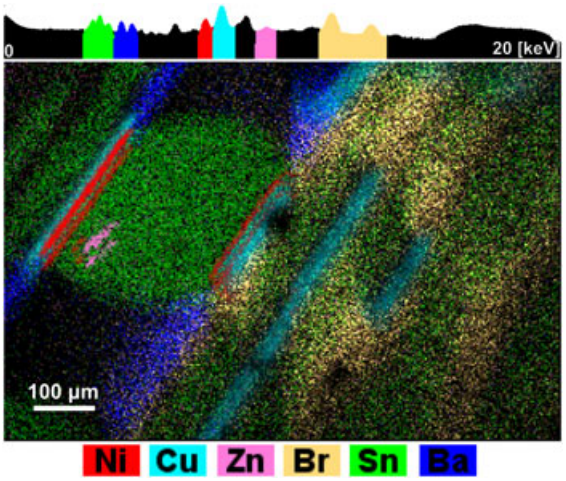

Figure 5. Multielemental XRF image of a RAM chip cross section measured with a laboratory X-ray tube using 8:1 optics. On top a logarithmic representation of a sum spectrum of the full-image area is presented. The image superposes the intensity distribution maps corresponding to characteristic lines of several elements: Ni Kα with red, Cu Kα with light blue, Zn Kβ with pink, all Br K lines with yellow, all Sn L lines with green, and Ba L lines with dark blue. The image is rendered with 2×2 sub-pixel division. A single pixel on the image corresponds to an area of $3 \times 3\,\mu m^2$. XRF, X-ray fluorescence.

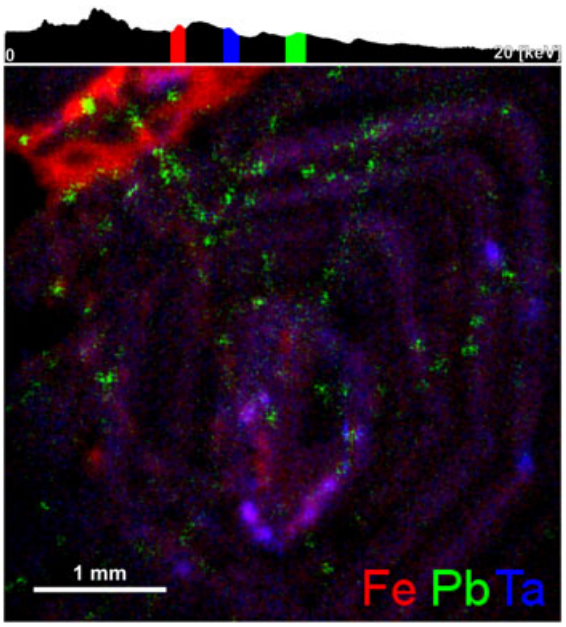

Figure 6. PIXE image of a Cassiterite sample with red, green, and blue channels assigned to the intensity of Fe Kα, As Kα, and Ta Lα fluorescence lines, respectively. On top a logarithmic representation of a sum spectrum of the full-image area is presented. The image is rendered with 4×4 sub-pixel division. A single pixel on the image corresponds to an area of $12 \times 12\,\mu m^2$. PIXE, particle-induced X-ray emission.

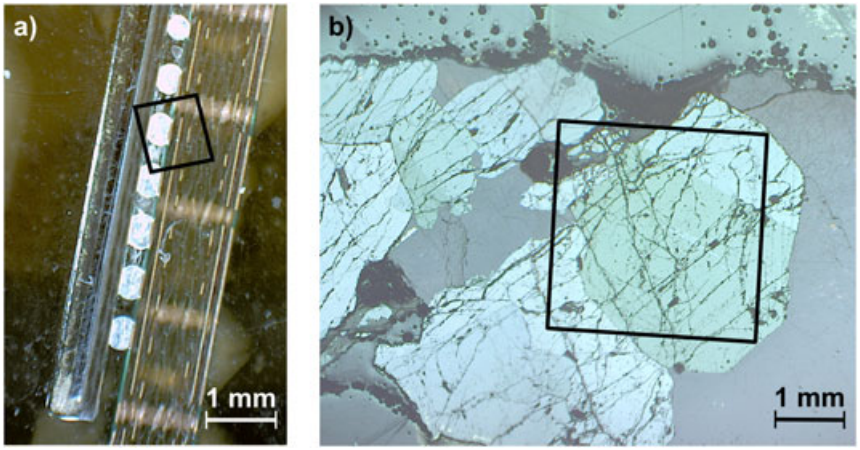

Figure 7. Optical images of: a) RAM cross-section sample, and b) Cassiterite sample. The Cassiterite image was acquired with the polarization microscope installed on the High-Speed PIXE beamline. The areas corresponding to X-ray emission images presented in Figures 5 and 6 are identified with black frames.

The improvement in SLcam® image quality is evident. With sub-pixel resolution, the pixelation effects are reduced and details below 10 μm can be clearly distinguished. Accordingly, the shape of the droplet boundary is well reproduced. Also a clear increase of the XRF intensity at the left slope of the droplet and shadowing in the center is visible. It should be noted that the beam footprint in TXRF measurements is in the range of millimeters[5]; thus, TXRF imaging with comparable resolution would not be possible in case of scanning methods[15,16].

Figure 5 shows an image of a RAM chip cross-section performed with an X-ray tube used for excitation. The measurement was performed with the 8:1 focusing optics, and the image was rendered with 2×2 sub-pixel division. The false color image was obtained by superposing color maps corresponding to the intensity of characteristic fluorescence lines of individual elements. Details with dimensions around 10 μm are clearly visible in Ni and Zn distributions.

The third example (see Figure 6) is a PIXE image of a mineral Cassiterite SnO_2 measured with 1:1 optics. Here the color image is obtained summing the red, green, and blue color maps corresponding to concentration of three different impurities. Small Pb inclusions of dimensions at the resolution limits are clearly visible. Ta and Fe can be seen in the form of shell-like structures. The Ta concentration everywhere in the crystal is below 1%, thus it can be classified as trace element.

The X-ray images of the RAM cross-section and Cassiterite can be compared with the optical images presented in Figure 7. Both optical images show a wider view on the samples; the area analyzed for X-ray emission is marked with black frames. For the case of XRF measurements at the laboratory, it should be noted that the X-ray image is skewed and stretched. This is a result of the unrestricted setup geometry in which both X-ray tube and SLcam® can be placed in any convenient position.

Conclusions

SLcam® can be used in various geometries at both XRF and PIXE installations; no focused excitation beam or sample movement are necessary. The detector equipped with the 1:1 optics with 20 μm channels is capable of full-field X-ray photon detection over an $12 \times 12\,mm^2$ sample area with a spatial resolution of 45 μm (11 LP/mm). Using 8:1 magnifying optics, a resolution of 5.4 μm (93 LP/mm) is reached over an image area of $1.5 \times 1.5\,mm^2$. Presented SLcam® performance is achieved because of the special fabrication of the polycapillary optics and sub-pixel algorithm. As a table top device, SLcam® in combination with a laboratory X-ray source offers outstanding resolution limits surpassing available micro-beam scanning solutions[17]. The unique properties of SLcam® make it ideal for, *e.g.* TXRF applications where detailed information on X-ray beam propagation and shadowing effects can be measured[16] and analyzed with appropriate models [18]. The first successful installation of SLcam® at PIXE facility was recently realized at High-Speed PIXE beamline at Ion Beam Center at Helmholtz-Zentrum Dresden-Rossendorf. The IFG Institute for Scientific Instruments GmbH continues research on a further improvement of obtainable resolution by reduction of the capillary channel diameter. The objective is to reach dimensions below 1 μm.

Acknowledgements

This work has been supported by Marie Curie Actions - Initial Training Networks (ITN) as an Integrating Activity Supporting Postgraduate Research with Internships in Industry and Training Excellence (SPRITE) under EC contract no. 317169. Thanks to M. Menzel and U. E. A. Fittschen, Universität Hamburg, Institut für Anorganische und Angewandte Chemie, for supply of the picoliter droplet.

References

[1] K. H. A. Janssens, F. C. V. Adams, A. Rindby, *Microscopic X-Ray Fluorescence Analysis*, Wiley, Chichester, **2002**.
[2] A. Bjeoumikhov, S. Bjeoumikhova, R. Wedell, New developments and applications of X-ray capillary optics, *Particle Systems Characterization* **2009**, *26*, 97–106.
[3] S. Majumdar, J. R. Peralta-Videa, H. Castillo-Michel, J. Hong, C. M. Rico, J. L. Gardea-Torresdey, Applications of synchrotron μ-XRF to study the distribution of biologically important elements in different environmental matrices: a review, *Analytica Chimica Acta* **2012**, *755*, 1–16.
[4] C. G. Ryan, PIXE and the nuclear microprobe: tools for quantitative imaging of complex natural materials, *Nuclear Instruments & Methods in Physics Research, Section B: Beam Interactions with Materials and Atoms* **2011**, *269*, 2151–2162.

[5] B. Beckhoff, R. Fliegauf, M. Kolbe, M. Müller, J. Weser, G. Ulm, Reference-free total reflection x-ray fluorescence analysis of semiconductor surfaces with synchrotron radiation, *Analytical Chemistry* **2007**, *79*, 7873–7882.
[6] O. Scharf, S. Ihle, I. Ordavo, V. Arkadiev, A. Bjeoumikhov, S. Bjeoumikhova, G. Buzanich, R. Gubzhokov, A. Güther, R. Hartmann, M. Kübacher, M. Lang, N. Langhoff, A. Liebel, M. Radtke, U. Reinholz, H. Riesemeier, H. Soltau, L. Strüder, A. F. Thünemann, R. Wedell, Compact pnCCD-based X-ray camera with high spatial and energy resolution: a color X-ray camera, *Analytical Chemistry* **2011**, *83*, 2532–2538.
[7] I. Ordavo, S. Ihle, V. Arkadiev, O. Scharf, H. Soltau, A. Bjeoumikhov, S. Bjeoumikhova, G. Buzanich, R. Gubzhokov, A. Günther, R. Hartmann, P. Holl, N. Kimmel, M. Kühbacher, M. Lang, N. Langhoff, A. Liebel, M. Radtke, U. Reinholz, H. Riesemeier, G. Schaller, F. Schopper, L. Strüder, C. Thamm, R. Wedell, A new pnCCD-based color X-ray camera for fast spatial and energy-resolved measurements, *Nuclear Instruments & Methods in Physics Research, Section A: Accelerators, Spectrometers, Detectors, and Associated Equipment* **2011**, *654*, 250–257.
[8] L. Strüder, U. Briel, K. Dennerl, R. Hartmann, E. Kendziorra, N. Meidinger, E. Pfeffermann, C. Reppin, B. Aschenbach, Bornemann, W., *et al*., The European photon imaging camera on XMM-Newton: the pn-CCD camera, *Astronomy and Astrophysics* **2001**, *365*, 18–26.
[9] S. H. Nowak, A. Bjeoumikhov, J. von Borany, J. Buchriegler, F. Munnik, M. Petric, M. Radtke, A. D. Renno, U. Reinholz, O. Scharf, R. Wedell **2015**, arXiv:1501.06825 [physics.ins-det].
[10] M. N. Boone, J. Garrevoet, P. Tack, O. Scharf, D. P. Cormode, D. V. Loo, E. Pauwels, M. Dierick, L. Vincze, L. V. Hoorebeke, High spectral and spatial resolution X-ray transmission radiography and tomography using a Color X-ray Camera, *Nuclear Instruments and Methods in Physics Research Section A: Accelerators, Spectrometers, Detectors and Associated Equipment* **2014**, *735*, 644–648.
[11] J. Donges, A. Rothkirch, T. Wroblewski, A. Bjeoumikhov, O. Scharf, I. Ordavo, S. Ihle, Energy dispersive X-ray diffraction imaging, *Materials Science Forum* **2013**, *772*, 21–25.
[12] A. Abboud, S. Send, R. Hartmann, L. Strüder, A. Savan, A. Ludwig, N. Zotov, U. Pietsch, Applications of an energy-dispersive pnCCD for X-ray reflectivity: investigation of interdiffusion in Fe-Pt multilayers, *Physica Status Solidi A: Applications and Materials Science* **2011**, *208*, 2601–2607.
[13] A. Bjeoumikhov, N. Langhoff, R. Wedell, V. Beloglazov, N. Lebed'ev, N. Skibina, New generation of polycapillary lenses: manufacture and applications, *X-Ray Spectrometry* **2003**, *32*, 172–178.
[14] H. Riesemeier, K. Ecker, W. Görner, B. R. Müller, M. Radtke, M. Krumrey, Layout and first XRF applications of the BAMline at BESSY II, *X-Ray Spectrometry* **2005**, *34*, 160–163.
[15] A. Kühn, O. Scharf, I. Ordavo, H. Riesemeier, U. Reinholz, M. Radtke, A. Berger, M. Ostermann, U. Panne, Pushing the limits for fast spatially resolved elemental distribution patterns, *Journal of Analytical Atomic Spectrometry* **2011**, *26*, 1986–1989.
[16] U. E. A. Fittschen, M. Menzel, O. Scharf, M. Radtke, U. Reinholz, G. Buzanich, V. M. Lopez, K. McIntosh, C. Streli, G. J. Havrilla, Observation of X-ray shadings in synchrotron radiation-total reflection X-ray fluorescence using a color X-ray camera, *Spectrochimica Acta, Part B: Atomic Spectroscopy* **2014**, *99*, 179–184.
[17] M. Haschke, *Laboratory Micro-X-Ray Fluorescence Spectroscopy*, Springer, Heidelberg, **2014**.
[18] S. H. Nowak, F. Reinhardt, B. Beckhoff, J.-Cl. Dousse, J. Szlachetko, Geometrical optics modelling of grazing incidence X-ray fluorescence of nanoscaled objects, *Journal of Analytical Atomic Spectrometry* **2013**, *28*, 689–696.